

with

$$\sum_T(q) = \sum_{i,j,p} \frac{C_{ijq}(\mathbf{p})}{[q - \omega_{ijq}(\mathbf{p})]^2} \times \text{Tr}[\Lambda_i(\mathbf{p}+\mathbf{q})\boldsymbol{\alpha} \cdot \hat{\lambda}\Lambda_j(\mathbf{p})\boldsymbol{\alpha} \cdot \hat{\lambda}]. \quad (17)$$

In the limit of small q^2 , the evaluation of (16) and (17) yields

$$\alpha^2 = \left[1 + \frac{2}{3\pi} e_0^2 \int \frac{p^2 dp}{(p^2 + m^2)^{3/2}} \left(\frac{3}{2} - \frac{1}{2} \frac{p^2}{p^2 + m^2} \right) \right]^{-1}, \quad (18)$$

which is identical to (6).

When two charged particles interact by exchange of a virtual transverse photon, their interaction is diminished by the factor $|\alpha|^2$, which is the reduced probability that a physical photon contains a bare photon.

Hence we conclude that both the longitudinal and transverse renormalization of the electromagnetic charge is given by the same expression. Equation (10) therefore gives the adjustment of the value of e in a metal environment.

If the above calculation were done by conventional Feynman-diagram techniques in quantum electrodynamics, Fig. 3 represents the diagrams which would yield the corrections to e calculated above in this paper.

Ultrashort-Pulse Generation by Q-Switched Lasers*

J. A. FLECK, JR.

Lawrence Radiation Laboratory, University of California, Livermore, California 94550

(Received 12 June 1969)

We have undertaken the complete temporal description of pulsed emission by a homogeneously broadened laser, including the effects of spontaneous emission, the detailed geometry of the laser cavity, and the variation of atomic polarization and level populations over wavelength distances. The model is based on traveling-wave equations which are derived from Maxwell's equations and solved in conjunction with boundary conditions imposed at the cavity mirrors. Thus, any direct assumptions concerning the nature of the laser's longitudinal mode structure is avoided. Variations in polarization and population over wavelength distances are treated by means of expansions in spatial Fourier series, having as fundamental a half optical wavelength. The Fourier series are truncated after the first harmonic. The treatment differs from earlier work in that the dephasing of the dipole moment is treated exactly without a rate-equation approximation. Spontaneous emission is simulated both as to spectrum and Gaussian character by including in the dipole equations stochastic shot-noise sources. The model equations are solved numerically, and results include the details of Q-switched pulse evolution from noise for both passive and active switching. In the case of an actively switched laser, the two-photon fluorescence intensity pattern has been calculated. It reveals a well-defined structure of subsidiary intensity maxima, even though subcavities are not assumed in the calculation. The pattern can be correlated directly with the emission pulse structure, and should vary from shot to shot. No single point in the pattern is suitable for a peak-to-background ratio determination. However, if the background is averaged over a distance in the fluorescing medium equal to twice the separation between cavity mirrors, the peak-to-background ratio would be ≈ 1.6 , indicating a highly uncorrelated spectrum.

INTRODUCTION

THE emission of radiation by lasers as a succession of pulses, under various conditions, has been a familiar phenomenon for some time.¹⁻¹⁰ Interest in

pulsed emission has heightened in recent years as the result of discoveries that solid-state lasers can emit trains of pulses having durations of the order of 10^{-12} sec, not only when mode locking is brought about,^{4,5} but even when mode control is not attempted.^{9,10} Much of the underlying detail of the resulting pulses cannot be resolved on a available oscilloscopes. As a consequence, experimenters have made use of nonlinear optical

* Work performed under the auspices of the U. S. Atomic Energy Commission.

¹ R. J. Collins, D. F. Nelson, A. L. Schawlow, W. Bond, C. G. B. Garrett, and W. Kaiser, *Phys. Rev. Letters* **5**, 303 (1960).

² L. E. Hargrove, R. L. Fork, and M. A. Pollock, *Appl. Phys. Letters* **5**, 4 (1964).

³ M. H. Crowell, *IEEE J. Quantum Electron.* **QE-1**, 12 (1965).

⁴ H. Mocker and R. J. Collins, *Appl. Phys. Letters* **7**, 270 (1965).

⁵ A. J. DeMaria, D. A. Stetser, and H. Heynau, *Appl. Phys. Letters* **8**, 174 (1966).

⁶ F. R. Nash, *IEEE J. Quantum Electron.* **QE-3**, 189 (1967).

⁷ P. W. Smith, *IEEE J. Quantum Electron.* **QE-3**, 627 (1967).

⁸ V. I. Malyshev, A. S. Markin, and A. A. Sychev, *Zh. Eksperim. i Teor. Fiz. Pis'ma v Redaktsiyu* **6**, 503 (1967) [English transl.: *Soviet Phys.—JETP Letters* **6**, 34 (1967)]; T. I. Kuznetsova, V. I. Malyshev, and A. S. Markin, *Zh. Eksperim. i Teor. Fiz.* **52**, 438 (1967) [English transl.: *Soviet Phys.—JETP* **25**, 286 (1967)].

⁹ M. A. Duguay, S. L. Shapiro, and P. M. Rentzepis, *Phys. Rev. Letters* **19**, 1014 (1967).

¹⁰ M. Bass and D. Woodward, *Appl. Phys. Letters* **12**, 275 (1968).

techniques for probing pulse structure.¹¹⁻¹⁴ These techniques yield data that is integrated over the entire duration of the pulsed emission, making it impossible to recover the complete details or the time history of the emission process. Care is thus required in interpreting the data for details of pulse structure.^{15,16} It would be useful to exhibit theoretically those details of pulsed laser emission which cannot be resolved either by means of oscilloscope or nonlinear optical data. One can, of course, interpret experimental data on the basis of simple *ad hoc* assumptions regarding the phasing of laser modes, but an understanding of the underlying emission processes must, in the final analysis, be based upon a dynamic model of the laser. In this paper, we have undertaken the derivation of a detailed model for describing short-pulse emission by lasers, and we have applied it, by solving the model equations numerically, to the generation of short pulses by a Q-switched laser operating both with and without a saturable absorber in the cavity. In applying this model, an attempt is made to follow the details of emission from initiation by spontaneous emission through nonlinear amplification and the depletion of gain. The cases listed above, however, are not intended to be an exhaustive list of possible applications for the methods described.

The conventional approach to laser theory has been to express the laser field as an expansion in a set of normal standing-wave modes appropriate to the laser cavity. Multimode theories of phase locking and pulse emission have been undertaken by a number of authors using this approach.¹⁷⁻²⁴ An alternative description of the laser field is based upon a direct solution of Maxwell's equations and reflection boundary conditions appropriate to the laser cavity. Such a treatment avoids any explicit assumptions regarding the longitudinal mode structure of the laser, and seems ideally suited to the time-domain description of pulse phenomena. This method yields equations for the field amplitudes which are of transport or traveling-wave type. Such a description will be referred to as a traveling wave or TW description.

The TW description is simplest to formulate and apply for the case of single-pass amplifiers and attenuators and one-wave ring lasers, since only one wave is involved. The TW method has been in use for some time for describing the effects of amplifiers and attenuators on radiation. Theories have been formulated both by neglecting the coherence of the polarization²⁵ (rate-equation theories) and by taking it into account²⁶⁻³³ (nonrate-equation theories). More recently, one-way ring lasers have been treated using a nonrate-equation TW description.^{34,35} The application of the TW method to a Fabry-Perot laser cavity is more complicated, partly because two opposite traveling waves are required, but also because the waves interfere. The TW method in a rate-equation approximation has been applied to Fabry-Perot lasers operating in a cw condition.^{36,37} In two earlier papers, time-dependent TW rate equations were used to describe the evolution of mode-locked pulses in passively switched lasers with Fabry-Perot cavities.^{38,39} Preliminary results based upon a nonrate-equation TW description, have been given for ordinary Q-switched lasers.^{40,41} The present paper will, in part, provide an elaboration of the results and methods discussed in Ref. 41.

Of the above references to applications of TW methods, only in Refs. 40 and 41 is the effect of spontaneous emission explicitly taken into account. The inclusion of spontaneous emission turns out to be crucial to gaining an understanding of the behavior of Q-switched solid-state lasers, since in amplifying systems which are not strongly affected by pumping what

¹¹ J. A. Armstrong, Appl. Phys. Letters **10**, 16 (1967).
¹² W. H. Glenn and M. J. Brienza, Appl. Phys. Letters **10**, 221 (1967).
¹³ H. P. Weber, J. Appl. Phys. **38**, 223 (1967); **39**, 6041 (1969).
¹⁴ J. A. Giordmaine, P. M. Rentzepis, S. L. Shapiro, and K. W. Wecht, Appl. Phys. Letters **11**, 216 (1967).
¹⁵ H. P. Weber, Phys. Letters **27A**, 321 (1968).
¹⁶ J. R. Klauder, M. A. Duguay, J. A. Giordmaine, and S. L. Shapiro, Appl. Phys. Letters **13**, 174 (1968).
¹⁷ W. E. Lamb, Jr., Phys. Rev. **134**, A1429 (1964).
¹⁸ M. J. DiDomenico, Jr., J. Appl. Phys. **35**, 388 (1965).
¹⁹ A. Yariv, J. Appl. Phys. **36**, 388 (1965).
²⁰ H. Statz and C. L. Tang, J. Appl. Phys. **36**, 3923 (1965).
²¹ C. A. Sacchi, G. Soncini, and O. Svelto, Nuovo Cimento **48**, 58 (1967).
²² V. S. Letokhov and V. N. Morozov, Zh. Eksperim. i Teor. Fiz. **52**, 1296 (1967) [English transl.: Soviet Phys.—JETP **25**, 862 (1967)].
²³ H. Haken and M. Pauthier, IEEE J. Quantum Electron. **QE-4**, 454 (1968).
²⁴ S. E. Schwartz, IEEE J. Quantum Electron. **QE-4**, 509 (1968).

²⁵ R. Bellman, G. Birnbaum, and W. G. Wagner, J. Appl. Phys. **34**, 780 (1963); L. M. Frantz and J. S. Nodvik, *ibid.* **34**, 2346 (1963); R. V. Ambartsumyan, N. G. Basov, V. S. Zuev, P. G. Kryukov, and V. S. Letokhov, IEEE J. Quantum Electron. **QE-2**, 436 (1966); the shaping of pulses by saturable absorbers is treated by E. Garmire and A. Yariv, *ibid.* **QE-3**, 222 (1967).
²⁶ J. P. Wittke and P. J. Warter, J. Appl. Phys. **34** (1963).
²⁷ F. T. Arecchi and R. Bonifacio, IEEE J. Quantum Electron. **QE-1**, 169 (1965).
²⁸ C. L. Tang and B. D. Silverman, in *Physics of Quantum Electronics*, edited by P. L. Kelley, B. Lax, and P. E. Tannenwald (McGraw-Hill Book Co., New York, 1966), p. 280.
²⁹ S. L. McCall and E. L. Hahn, Phys. Rev. Letters **8**, 908 (1967).
³⁰ W. G. Wagner, H. A. Haus, and K. T. Gustafson, IEEE J. Quantum Electron. **QE-4**, 267 (1968).
³¹ J. A. Armstrong and E. Courtens, IEEE J. Quantum Electron. **QE-4**, 411 (1968); J. A. Armstrong and E. Courtens, *ibid.* **QE-5**, 249 (1969).
³² F. A. Hopf and M. O. Scully, Phys. Rev. **179**, 399 (1969).
³³ R. Bonifacio and L. Narducci, Nuovo Cimento (to be published).
³⁴ C. L. Tang and H. Statz, J. Appl. Phys. **39**, 31 (1968).
³⁵ H. Risken and K. Nummedal, J. Appl. Phys. **39**, 4662 (1968).
³⁶ L. A. Ostrovskii and I. E. Yakubovich, Zh. Eksperim. i Teor. Fiz. **46**, 963 (1963) [English transl.: Soviet Phys.—JETP **19**, 656 (1965)].
³⁷ V. M. Aruthunyan, Zh. Eksperim. i Teor. Fiz. **53**, 183 (1968) [English transl.: Soviet Phys.—JETP **26**, 125 (1968)]; this reference also treats aspects of the time-dependent problem.
³⁸ J. A. Fleck, Jr., Appl. Phys. Letters **12**, 178 (1968).
³⁹ J. A. Fleck, Jr., J. Appl. Phys. **39**, 3318 (1968).
⁴⁰ J. A. Fleck, Jr., Phys. Rev. Letters **21**, 131 (1968).
⁴¹ J. A. Fleck, Jr., Appl. Phys. Letters **13**, 365 (1968).

comes out depends very strongly on what is put in. For systems in which pumping plays an important role, the influence of spontaneous emission should be less important. In Refs. 34 and 35, instabilities are reported which depend on pumping. These results should be applicable to the continuous pulsing of gas lasers,^{6,7} but not to the cases examined here.

The method which we use for deriving field amplitude equations is based on a direct application of Maxwell's equations rather than on a second-order wave equation. In Sec. I, a set of exact TW equations is derived without making a slowly varying envelope approximation. These equations could be used for describing the amplification of ultrashort pulses, say, from 1 to 100 wavelengths long over centimeter distances, but would be impractical for numerical use in describing amplification inside a laser cavity where amplification paths are far longer. In Sec. II, it is shown by means of a slowly varying envelope approximation and a rate-equation approximation that the equations derived in Sec. I contain small phase modulation effects which can be neglected for the cases of interest in this paper. In Sec. III, a slowly varying envelope approximation is applied to the equations derived in Sec. I, and it is shown that the interference between the two oppositely traveling waves in a cavity creates a variation in the polarization and population difference, over a distance of a half-wavelength, which can have an important effect on the slowly varying field amplitudes. The rapid local spatial variation in polarization and population difference can be treated either by means of Fourier expansions with a half-wavelength as fundamental, as is done in Sec. III, or by sampling these variables at discrete points over a half-wavelength distance, as is shown in Sec. IV. The remaining analysis in the paper is based on a truncated Fourier expansion. Section V is devoted to a discussion of the fluctuating dipole model of spontaneous emission which is similar to Langevin source models which have been employed in the noise analysis of single-mode lasers.⁴² The numerical methods used are discussed in Sec. VI, and numerical results are presented in Sec. VII.

I. BASIC EQUATIONS

Whereas most treatments of laser phenomena begin with the consideration of a second-order wave equation, we shall find it convenient to deal directly with the Maxwell field equations, which for a plane-polarized beam can be written as

$$\frac{\epsilon}{c} \frac{\partial E_x}{\partial t} = -\frac{\partial H_y}{\partial z} - \frac{4\pi}{c} \frac{\partial P}{\partial t} - \frac{4\pi}{c} \sigma E_x, \quad (1.1a)$$

$$\frac{\mu}{c} \frac{\partial H_y}{\partial t} = -\frac{\partial E_x}{\partial z}. \quad (1.1b)$$

Here the permittivity ϵ and the magnetic permeability μ refer to a dispersionless host medium, σ is a conductivity, P is a polarization which characterizes the active atoms which may be either amplifying or absorbing, and E_x and H_y are the electric and magnetic field components. Equations (1.1) can be rewritten in terms of variables $\epsilon^{1/2}E_x$ and $\mu^{1/2}H_y$ as follows:

$$\frac{(\epsilon\mu)^{1/2}}{c} \frac{\partial}{\partial t} (\epsilon^{1/2}E_x) = -\frac{\partial(\mu^{1/2}H_y)}{\partial z} - \frac{4\pi\mu^{1/2}}{c} \frac{\partial P}{\partial t} - \frac{4\pi}{c} \left(\frac{\mu}{\epsilon}\right)^{1/2} \sigma (\epsilon^{1/2}E_x), \quad (1.2a)$$

$$\frac{(\epsilon\mu)^{1/2}}{c} \frac{\partial}{\partial z} (\mu^{1/2}H_y) = -\frac{\partial}{\partial z} (\epsilon^{1/2}E_x). \quad (1.2b)$$

We next introduce variables E^+ and E^- which satisfy

$$E^+ = \epsilon^{1/2}E_x + \mu^{1/2}H_y, \quad (1.3a)$$

$$E^- = \epsilon^{1/2}E_x - \mu^{1/2}H_y, \quad (1.3b)$$

$$\epsilon^{1/2}E_x = \frac{1}{2}(E^+ + E^-), \quad (1.3c)$$

$$\mu^{1/2}H_y = \frac{1}{2}(E^+ - E^-). \quad (1.3d)$$

If we first add Eqs. (1.2a) and (1.2b) and then subtract Eq. (1.2b) from Eq. (1.2a), we obtain the following first-order equations satisfied by E^+ and E^- :

$$\frac{\eta}{c} \frac{\partial E^+}{\partial t} + \frac{\partial E^+}{\partial z} = -\frac{4\pi\mu^{1/2}}{c} \frac{\partial P}{\partial t} - \frac{2\pi\sigma}{c} \left(\frac{\mu}{\epsilon}\right)^{1/2} (E^+ + E^-), \quad (1.4a)$$

$$\frac{\eta}{c} \frac{\partial E^-}{\partial t} - \frac{\partial E^-}{\partial z} = -\frac{4\pi\mu^{1/2}}{c} \frac{\partial P}{\partial t} - \frac{2\pi\sigma}{c} \left(\frac{\mu}{\epsilon}\right)^{1/2} (E^+ + E^-), \quad (1.4b)$$

where $\eta = (\epsilon\mu)^{1/2}$ is the refractive index of the host medium. Maxwell's equations are thus reduced to a pair of first-order transport equations.

To illustrate the significance of E^+ and E^- , we derive some elementary relations from Eqs. (1.3) and (1.4). First, the energy density u of the electromagnetic field can be expressed in terms of E^+ and E^- as

$$u = \frac{1}{8\pi} (\epsilon E_x^2 + \mu H_y^2) = \frac{1}{16\pi} (E^{+2} + E^{-2}), \quad (1.5)$$

where use has been made of relations (1.3c) and (1.3d). Thus, E^{+2} and E^{-2} contribute additively to the energy density of the field. We can express the magnitude S

⁴² H. Risken, Z. Physik **186**, 85 (1965); J. A. Fleck, Jr., J. Appl. Phys. **37**, 188 (1966).

of the Poynting vector as

$$S = \frac{c}{4\pi} E_x H_y = \frac{c}{16\pi\eta} (E^{+2} - E^{-2}). \quad (1.6)$$

Here S is expressed as the net difference between the energy flux traveling to the right and to the left. Consider next the propagation of a plane wave through a medium without polarization or conductivity, which requires setting the right-hand sides of Eqs. (1.4) equal to zero. If we assume the wave is propagated to the right, E^+ and E^- satisfy

$$\frac{\eta}{c} \frac{\partial E^+}{\partial t} + \frac{\partial E^+}{\partial z} = 0, \quad (1.7a)$$

$$E^- = 0. \quad (1.7b)$$

From (1.7b) $\epsilon^{1/2} E_x = \mu^{1/2} H_y$ and from (1.7a) $E_x = f(t - \eta z/c)$, where $E_x(0, t) = f(t)$. Let us consider finally the case of a medium without polarization but with a conductivity. Equations (1.4) become

$$\frac{\eta}{c} \frac{\partial E^+}{\partial t} + \frac{\partial E^+}{\partial z} = -\frac{2\pi\sigma}{c} \left(\frac{\mu}{\epsilon}\right)^{1/2} (E^+ + E^-), \quad (1.8a)$$

$$\frac{\eta}{c} \frac{\partial E^-}{\partial t} - \frac{\partial E^-}{\partial z} = -\frac{2\pi\sigma}{c} \left(\frac{\mu}{\epsilon}\right)^{1/2} (E^+ + E^-). \quad (1.8b)$$

Even if we consider a wave proceeding to the right, it is no longer possible to set $E^- = 0$, since E^- and E^+ are coupled. Let us take then E^+ and E^- in the form

$$E^+ = \mathcal{E}^+(z, t) e^{i(\omega t - kz)}, \quad (1.9a)$$

$$E^- = \mathcal{E}^-(z, t) e^{i(\omega t - kz)}, \quad (1.9b)$$

where $k = \eta\omega/c$ and \mathcal{E}^+ and \mathcal{E}^- vary slowly compared to the exponentials. Substituting (1.9b) into (1.8b), one obtains

$$\frac{\eta}{c} \frac{\partial \mathcal{E}^-}{\partial t} - \frac{\partial \mathcal{E}^-}{\partial z} + 2ik \mathcal{E}^- = -\Lambda (\mathcal{E}^+ + \mathcal{E}^-), \quad (1.10)$$

where

$$\Lambda = (2\pi\sigma/c) (\mu/\epsilon)^{1/2}. \quad (1.11)$$

Since \mathcal{E}^- is slowly varying, one can neglect the derivatives on the left-hand side of (1.10) and write

$$\mathcal{E}^- \approx -\Lambda \mathcal{E}^+ / (\Lambda + 2ik) \approx i\Lambda \mathcal{E}^+ / 2k, \quad (1.12)$$

if $k \gg \Lambda$. Substituting (1.12) into (1.8a), we obtain

$$\frac{\eta}{c} \frac{\partial \mathcal{E}^+}{\partial t} + \frac{\partial \mathcal{E}^+}{\partial z} = -\left(\Lambda + \frac{i\Lambda^2}{2k}\right) \mathcal{E}^+, \quad (1.13)$$

with a solution

$$\mathcal{E}^+ = f(t - \eta z/c) \exp[-(\Lambda + i\Lambda^2/2k)z]. \quad (1.14)$$

Expression (1.14) exhibits an exponential falloff in field amplitude with distance and a shift in wave number $\Delta k = \Lambda^2/2k$. This shift in wave number, of course, agrees with what could be derived from the dispersion relation for Eqs. (1.1) with $P = 0$,

$$\eta^2 \omega^2 / c^2 - k^2 + 4\pi\sigma\omega i / c^2 = 0, \quad (1.15)$$

in the limit $k \gg \Lambda$.

We turn our attention next to equations satisfied by the polarization P . For a two-level system, P is given by

$$P = N\bar{\mu}(\rho_{12} + \rho_{21}), \quad (1.16)$$

where N is the number of active atoms per unit volume, $\bar{\mu}$ is the mean component of the atomic dipole matrix element projected along the direction of the polarization of the field, and ρ_{12} and ρ_{21} are the off-diagonal elements of a two-level density matrix which satisfy

$$\rho_{21} = \rho_{12}^*, \quad (1.17a)$$

$$\frac{\partial \rho_{12}}{\partial t} + (-i\omega + T_2^{-1})\rho_{12} = -\left(\frac{i}{\hbar}\right) \bar{\mu}(\rho_{11} - \rho_{22}) E_x. \quad (1.17b)$$

$$\begin{aligned} \frac{\partial}{\partial t} (\rho_{22} - \rho_{11}) &= T_1^{-1} [(\rho_{22}^0 - \rho_{11}^0) - (\rho_{22} - \rho_{11})] \\ &+ \left(\frac{2i}{\hbar}\right) \bar{\mu}(\rho_{12} - \rho_{21}) E_x. \end{aligned} \quad (1.17c)$$

In Eqs. (1.17), T_2 and T_1 are the longitudinal and transverse relaxation times, ω is the circular transition frequency, ρ_{22} and ρ_{11} are the probabilities of occupying the upper and lower states, and $N(\rho_{22}^0 - \rho_{11}^0) = n^0$ is the steady-state population difference which would prevail in the absence of laser radiation. If we introduce a complex polarization $P_c = N\bar{\mu}\rho_{12}$ and a population difference variable $n = N(\rho_{22} - \rho_{11})$, Eqs. (1.4) and (1.17) become

$$\begin{aligned} \frac{\eta}{c} \frac{\partial E^+}{\partial t} + \frac{\partial E^+}{\partial z} &= \frac{4\pi\mu^{1/2}}{c} [(-i\omega + T_2^{-1})P_c + (i\omega + T_2^{-1})P_c^*] \\ &- \frac{2\pi\sigma}{c} \left(\frac{\mu}{\epsilon}\right)^{1/2} (E^+ + E^-), \end{aligned} \quad (1.18a)$$

$$\begin{aligned} \frac{\eta}{c} \frac{\partial E^-}{\partial t} - \frac{\partial E^-}{\partial z} &= \frac{4\pi\mu^{1/2}}{c} [(-i\omega + T_2^{-1})P_c + (i\omega + T_2^{-1})P_c^*] \\ &- \frac{2\pi\sigma}{c} \left(\frac{\mu}{\epsilon}\right)^{1/2} (E^+ + E^-), \end{aligned} \quad (1.18b)$$

$$\frac{\partial P_c}{\partial t} + (-i\omega + T_2^{-1})P_c = \left(\frac{i}{\hbar}\right)\bar{\mu}^2 \frac{n(E^+ + E^-)}{2\epsilon^{1/2}}, \quad (1.18c)$$

$$\frac{\partial n}{\partial t} = T_1^{-1}(n^0 - n) + \frac{2i}{\hbar}(P_c - P_c^*) \frac{E^+ + E^-}{2\epsilon^{1/2}}. \quad (1.18d)$$

The elimination of the derivatives of P on the right-hand side of Eqs. (1.4) is made possible by the fact that the right-hand side of Eq. (1.18c) is pure imaginary.

Equations (1.18) contain no approximations and are in a form convenient for numerical integration. In general, both E^+ and E^- must be retained even if it is known from symmetry considerations that wave motion proceeds in only one direction. The presence of ω in Eq. (1.18c), however, requires that the detailed optical-wave motion be followed. This is both impractical and, as it turns out, unnecessary in the cases of interest to us, although Eqs. (1.18) might be useful in studying the amplification of subpicosecond pulses. We must therefore look for ways of separating optical carrier waves from E^+ and E^- , which we shall do in Sec. III.

It will be convenient to renormalize the variables in Eqs. (1.18). We make the replacement

$$E^\pm \rightarrow (c/16\pi\eta\hbar\omega)^{1/2}E^\pm \quad (1.19)$$

by multiplying Eqs. (1.18a)–(1.18c) through by $(c/16\pi\eta\hbar\omega)^{1/2}$ and defining P' by

$$P' = i(4\pi\omega/c)(\mu c/16\pi\eta\hbar\omega)^{1/2}P_c. \quad (1.20)$$

We also drop the conductivity terms in Eqs. (1.18), since no further use will be made of them. Equations (1.18) become

$$\frac{\eta}{c} \frac{\partial E^+}{\partial t} + \frac{\partial E^+}{\partial z} = -(1+i\delta)P' + \text{c.c.}, \quad (1.21a)$$

$$\frac{\eta}{c} \frac{\partial E^-}{\partial t} - \frac{\partial E^-}{\partial z} = -(1+i\delta)P' + \text{c.c.}, \quad (1.21b)$$

$$\frac{\partial P'}{\partial t} + (-i\omega + T_2^{-1})P' = -\frac{1}{2}T_2^{-1}\sigma_0 n(E^+ + E^-), \quad (1.21c)$$

$$\frac{\partial n}{\partial t} = T_1^{-1}(n^0 - n) + 4(P' + P'^*)(E^+ + E^-), \quad (1.21d)$$

where we have introduced

$$\delta = (\omega T_2)^{-1} \quad (1.22)$$

and the cross section at line center for stimulated emission or absorption,

$$\sigma_0 = (4\pi\bar{\mu}^2\omega T_2/\hbar c)(\mu/\epsilon)^{1/2}. \quad (1.23)$$

II. DISPERSIVE EFFECTS

Before going on to a detailed treatment of Eqs. (1.21), we shall isolate and discuss a pair of dispersive effects

so that they do not need to be considered later.⁴³ For simplicity, let us consider a single wave moving to the right. Again we take

$$\begin{aligned} E^+ &= \mathcal{E}^+(z, t)e^{i(\omega t - kz)} + \text{c.c.}, \\ E^- &= \mathcal{E}^-(z, t)e^{i(\omega t - kz)} + \text{c.c.} \end{aligned} \quad (2.1)$$

If we ignore the space and time dependence of n , \mathcal{E}^+ , and \mathcal{E}^- , we can solve Eq. (1.21c) in a rate-equation approximation, which should be accurate enough for our purposes here:

$$P' = -\frac{1}{2}\sigma_0 n(\mathcal{E}^+ e^{i(\omega t - kz)} + \mathcal{E}^- e^{i(\omega t - kz)}). \quad (2.2)$$

Substituting this result into Eqs. (1.21a) and (1.21b), we have

$$\frac{\eta}{c} \frac{\partial \mathcal{E}^+}{\partial t} + \frac{\partial \mathcal{E}^+}{\partial z} = \frac{1}{2}\sigma_0 n(1+i\delta)(\mathcal{E}^+ + \mathcal{E}^-), \quad (2.3a)$$

$$\frac{\eta}{c} \frac{\partial \mathcal{E}^-}{\partial t} - \frac{\partial \mathcal{E}^-}{\partial z} + 2ik\mathcal{E}^- = \frac{1}{2}\sigma_0 n(1+i\delta)(\mathcal{E}^+ + \mathcal{E}^-). \quad (2.3b)$$

If in Eq. (2.3b) we neglect the total derivative and $n\sigma_0$ in comparison with $k\mathcal{E}^-$, we have

$$\mathcal{E}^- \approx -(i/4k)n\sigma_0(1+i\delta)\mathcal{E}^+. \quad (2.4)$$

Since in general $n\sigma_0 \ll k$, $|\mathcal{E}^-|$ will thus be small compared with $|\mathcal{E}^+|$. Substituting this result into Eq. (2.3a),

$$\begin{aligned} \frac{\eta}{c} \frac{\partial \mathcal{E}^+}{\partial t} + \frac{\partial \mathcal{E}^+}{\partial z} &= \frac{1}{2}\sigma_0 n(1+i\delta) \left(1 - \frac{i}{4k}n\sigma_0(1+i\delta)\right) \mathcal{E}^+ \\ &\cong \frac{1}{2}\sigma_0 n[1+i(\delta - n\sigma_0/4k)] \mathcal{E}^+. \end{aligned} \quad (2.5)$$

The resulting gain is complex, with the imaginary part of the gain leading to a change in wave number,

$$\Delta k = \frac{1}{2}\sigma_0 n[(\omega T_2)^{-1} - n\sigma_0/4k], \quad (2.6)$$

or, equivalently, a change in refractive index

$$\Delta \eta = (c\sigma_0 n/2\omega)[(\omega T_2)^{-1} - n\sigma_0/4k]. \quad (2.7)$$

For ruby, the maximum possible value of $n\sigma_0$ is ≈ 0.4 , T_2 at room temperature is $\sim 10^{-12}$ sec,⁴⁴ and $\omega = 2.7 \times 10^{15}$ rad/sec. Thus, the first term in the brackets in Eqs. (2.6) and (2.7) dominates, and we have

$$\begin{aligned} \Delta k &\approx 10^{-4} \text{ cm}^{-1}, \\ \Delta \omega &\approx 10^6 \text{ rad/sec}, \\ \Delta \eta &\approx 10^{-9}. \end{aligned}$$

Granted that variations of n could produce phase modulations, it is evident from the preceding numbers that such effects would be entirely negligible in the solid-state laser materials of interest. The value of

⁴³ For further discussion of dispersive effects in pulse amplification, the reader is referred to Ref. 31.

⁴⁴ D. E. McCumber and M. D. Sturge, J. Appl. Phys. 34, 1682 (1963).

$(\omega T_2)^{-1}$ is not known for the dyes used as switches. If it were as large as 1.0, then $\Delta\omega$ could be of the order of 10^9 rad/sec. Thus, every time that a pulse bleaches through a dye its circular frequency would be swept by this amount. But clearly an enormous number of bleaching passes would be required to produce the chirping effects which have been observed.⁴⁵ In the light of the preceding discussion, we can treat E^+ and E^- to a very good approximation as waves moving, respectively, to the right and to the left, and we can set $\delta=0$ in Eqs. (1.21a) and (1.21b).

III. DERIVATION OF TW EQUATIONS BY USE OF FOURIER SERIES

We now seek to express solutions to Eqs. (1.21) in the form

$$E^+(z,t) = \mathcal{E}^+(z,t)e^{i(\omega t - kz)} + \text{c.c.}, \quad (3.1a)$$

$$E^-(z,t) = \mathcal{E}^-(z,t)e^{i(\omega t + kz)} + \text{c.c.}, \quad (3.1b)$$

$$P'(z,t) = \rho(z,t)e^{i\omega t}, \quad (3.1c)$$

where $\mathcal{E}^+(z,t)$, $\mathcal{E}^-(z,t)$, vary slowly in comparison with the exponentials.

If we substitute expressions (3.1) into Eqs. (1.21a) and (1.21b), setting $\delta=0$, we must have

$$\frac{\eta}{c} \frac{\partial \mathcal{E}^+}{\partial t} + \frac{\partial \mathcal{E}^+}{\partial z} = -\langle \rho e^{ikz} \rangle, \quad (3.2a)$$

$$\frac{\eta}{c} \frac{\partial \mathcal{E}^-}{\partial t} - \frac{\partial \mathcal{E}^-}{\partial z} = -\langle \rho e^{-ikz} \rangle. \quad (3.2b)$$

The quantities which appear on the right-hand sides of Eqs. (3.2) may undergo rapid spatial variations. It is therefore only the spatial averages of these quantities taken over a few wavelengths, indicated by brackets, which contribute to the slowly varying functions \mathcal{E}^+ and \mathcal{E}^- . If we substitute expressions (3.1) into (1.21b) and (1.21c) and make a rotating wave approximation, the result is

$$\frac{\partial \rho}{\partial t} + T_2^{-1} \rho = -\frac{1}{2} T_2^{-1} \sigma_0 n (\mathcal{E}^+ e^{-ikz} + \mathcal{E}^- e^{ikz}), \quad (3.3a)$$

$$\frac{\partial n}{\partial t} = T_1^{-1} (n^0 - n) + 4(\rho \mathcal{E}^{+*} e^{ikz} + \rho \mathcal{E}^{-*} e^{-ikz} + \text{c.c.}). \quad (3.3b)$$

Unfortunately, there is no simple way of handling the exponentials which appear in Eqs. (3.3) in time-dependent problems. The physical reason why they need to be considered is that the presence of oppositely directed waves leads to a quasistanding-wave pattern and a variation in the field intensity over a half-wavelength distance. This spatial behavior of the field and intensity can in turn cause important variations in the

population difference and polarization over similar distances.⁴⁶

One method of treating the exponentials in Eqs. (3.3) is to make use of the Fourier series expansions for ρ and n ,

$$\rho(z,t) = e^{-ikz} \sum_{p=0}^{\infty} \rho_p^+ e^{-i2pkz} + e^{ikz} \sum_{p=0}^{\infty} \rho_p^- e^{i2pkz}, \quad (3.4a)$$

$$n(z,t) = \bar{n} + \sum_{p=1}^{\infty} (n_p e^{-i2pkz} + \text{c.c.}). \quad (3.4b)$$

If expressions (3.4) are substituted into Eqs. (3.2) and (3.3) and the orthogonality of the terms of the Fourier series is made use of, the following coupled equations for \mathcal{E}^+ , \mathcal{E}^- , ρ_p^+ , ρ_p^- , n_p , and \bar{n} result:

$$\frac{\eta}{c} \frac{\partial \mathcal{E}^+}{\partial t} + \frac{\partial \mathcal{E}^+}{\partial z} = -\rho_0^+, \quad (3.5a)$$

$$\frac{\eta}{c} \frac{\partial \mathcal{E}^-}{\partial t} - \frac{\partial \mathcal{E}^-}{\partial z} = -\rho_0^-, \quad (3.5b)$$

$$\frac{\partial \rho_p^+}{\partial t} + T_2^{-1} \rho_p^+ = -\frac{1}{2} T_2^{-1} \sigma_0 (n_p \mathcal{E}^+ + n_{p+1} \mathcal{E}^-) + S^+ \delta_{p0}, \quad (3.5c)$$

$$\frac{\partial \rho_p^-}{\partial t} + T_2^{-1} \rho_p^- = -\frac{1}{2} T_2^{-1} \sigma_0 (n_p^* \mathcal{E}^- + n_{p+1}^* \mathcal{E}^+) + S^- \delta_{p0}, \quad (3.5d)$$

$$\frac{\partial n_p}{\partial t} + T_1^{-1} n_p = 4(\rho_{p-1}^+ \mathcal{E}^{-*} + \rho_p^+ \mathcal{E}^{+*} + \rho_{p-1}^{-*} \mathcal{E}^+ + \rho_p^{-*} \mathcal{E}^-), \quad (3.5e)$$

$$\frac{\partial \bar{n}}{\partial t} + T_1^{-1} (n - n^0) = 4(\mathcal{E}^{-*} \rho_0^- + \mathcal{E}^{+*} \rho_0^+ + \text{c.c.}), \quad (3.5f)$$

$$p = 1, 2, \dots$$

Phenomenological source terms have been added to Eqs. (3.5c) and (3.5d) for $p=0$. These source terms represent the effect of spontaneous emission, and will be commented upon in Sec. V. It is evident from the coupling of Eqs. (3.5) that short-range spatial variations in $n(z,t)$ and $\rho(z,t)$ can influence the slowly varying functions \mathcal{E}^+ and \mathcal{E}^- .

Equations (3.5) contain a complete description of a homogeneously broadened laser. It is not known in general how many terms are needed in the summations (3.4) to achieve satisfactory accuracy. Obviously, terms through $p=1$ need to be retained if the short-range spatial variation of the atomic variables is to be described at all. What is required beyond this should depend on the case in question. This much can be said. The number of terms needed is not necessarily a func-

⁴⁵ E. B. Treacy, Phys. Letters 28A, 34 (1968).

⁴⁶ C. L. Tang, H. Statz, and G. de Mars, J. Appl. Phys. 34, 2289 (1963).

tion of the degree of nonlinearity of the absorption or amplification processes, but should be influenced more by the relative strength of the two crossing beams and the importance of pumping and relaxation processes in restoring depleted population differences. It should be further emphasized that the higher-order details of this "spatial hole burning" are important only insofar as they influence through coupling those lower-order components which directly affect the field. It may be helpful to draw an analogy between the present problem and that of solving the Boltzmann equation for one-dimensional neutron or photon transport.⁴⁷ In the latter cases it is customary to express the specific intensity as a polynomial expansion in the cosine of the angle which specifies the particle direction. The lowest-order expansion is linear in the angular variable and leads to diffusion theory. While such a description does not allow for much angular definition in the specific intensity, experience has always been that the resulting calculations of particle densities are far better than the detail of angular description would seem to warrant. The analog of diffusion theory in the case of Eqs. (3.5) involves a neglect of terms past $p=1$. It would be hoped that a $p=1$ expansion would similarly allow reasonable accuracy in the determination of the fields and spatially averaged population differences. In any case, in the calculations which are described in Sec. VII the value of $|n_1|/\bar{n}$, which may be some indication of the importance of higher-order expansion terms, generally stays below 0.1 and only very briefly gets as high as 0.5 in the description of saturable absorption.

IV. DERIVATION OF TW EQUATIONS BY SAMPLING

There is an additional way of reducing Eqs. (3.2) and (3.3) to a finite number of equations capable of numerical solution. One can write Eqs. (3.3a) and (3.3b) for discrete values of z , sampled over a half-wavelength distance, and then express the spatial averages which appear in Eqs. (3.2) as discrete sums, determined by a numerical integration formula. Let us write

$$\rho e^{ikz} = \rho^+, \quad (4.1a)$$

$$\rho e^{-ikz} = \rho^-. \quad (4.1b)$$

From Eq. (3.3a) we obtain the following equations for ρ^+ and ρ^- :

$$\frac{\partial \rho^+}{\partial t} + T_2^{-1} \rho^+ = -\frac{1}{2} T_2^{-1} \sigma_0 n (\mathcal{E}^+ + \mathcal{E}^- e^{2ikz}), \quad (4.2a)$$

$$\frac{\partial \rho^-}{\partial t} + T_2^{-1} \rho^- = -\frac{1}{2} T_2^{-1} \sigma_0 n (\mathcal{E}^- + \mathcal{E}^+ e^{-2ikz}), \quad (4.2b)$$

⁴⁷ S. Chandrasekhar, *Radiative Transfer* (Clarendon Press, Oxford, 1950); B. Davison, *Neutron Transport Theory* (Clarendon Press, Oxford, 1957).

and, in terms of the variables (4.1), Eq. (3.3b) becomes

$$\frac{\partial n}{\partial t} = T_2^{-1} (n^0 - n) + 4(\rho^+ \mathcal{E}^{+*} + \rho^- \mathcal{E}^{-*} + \text{c.c.}). \quad (4.3)$$

If we divide the distance between some point z and $z + \frac{1}{2}\lambda$ into M equal intervals, where for convenience z is taken to be an integral number of wavelengths, then at the discrete points which separate these intervals Eqs. (4.2) and (4.3) become

$$\frac{\partial \rho_p^+}{\partial t} + T_2^{-1} \rho_p^+ = -\frac{1}{2} T_2^{-1} \sigma_0 n_p (\mathcal{E}^+ + \mathcal{E}^- e^{2\pi i p/M}), \quad (4.4a)$$

$$\frac{\partial \rho_p^-}{\partial t} + T_2^{-1} \rho_p^- = -\frac{1}{2} T_2^{-1} \sigma_0 n_p (\mathcal{E}^- + \mathcal{E}^+ e^{-2\pi i p/M}), \quad (4.4b)$$

$$\frac{\partial n_p}{\partial t} = T_2^{-1} (n^0 - n_p) + 4(\rho_p^+ \mathcal{E}^{+*} + \rho_p^- \mathcal{E}^{-*} + \text{c.c.}), \quad (4.4c)$$

$$p = 1, 2, \dots, M,$$

where $n_p(z, t) = n(z + p\lambda/2M, t)$. If in the averages appearing in Eqs. (3.2) we treat each value of p as having equal weight, i.e., the averages are evaluated according to a trapezoidal numerical integration rule, then Eqs. (3.2) can be written as

$$-\frac{\eta}{c} \frac{\partial \mathcal{E}^+}{\partial t} + \frac{\partial \mathcal{E}^+}{\partial z} = -\frac{1}{M} \sum_{p=1}^M \rho_p^+, \quad (4.4d)$$

$$-\frac{\eta}{c} \frac{\partial \mathcal{E}^-}{\partial t} - \frac{\partial \mathcal{E}^-}{\partial z} = -\frac{1}{M} \sum_{p=1}^M \rho_p^-. \quad (4.4e)$$

Equations (4.4), which constitute the discrete sampling TW equations, are no more formidable than the Fourier series TW equations derived in Sec. III, and in some ways are actually simpler to treat. We shall not deal further with Eqs. (4.4) in this paper. We have only included them here to indicate a possible alternative to the Fourier series TW method.

Before leaving the subject, however, we shall venture a comment on the relative accuracy of Eqs. (4.4) and (3.5) for a given total number of equations used in either system. A reasonable estimate would be that if the maximum value of p used in Eqs. (3.5) were p_{\max} , then comparable accuracy in using Eqs. (4.4) would require a total of

$$M = 2p_{\max} + 1$$

sampling points, based on the simple fact that the same number of variables (or amount of information) characterizes the medium in both cases.

V. TREATMENT OF SPONTANEOUS EMISSION

The phenomenological source terms S^+ and S^- which appear in Eqs. (3.5a) and (3.5b) are meant to create a fluctuating contribution to the dipole moment

which is independent of \mathcal{E}^+ and \mathcal{E}^- . This fluctuating contribution to the dipole moment in turn acts as a spontaneous emission source to Eqs. (3.5a) and (3.5b). The latter should be Gaussian with a Lorentz spectrum and a frequency width equal to the fluorescence line-width.⁴⁸ The following forms for S^+ and S^- meet the above requirements:

$$S^\pm(z_j, t) = A_s \sum_{m'=0}^m \exp(i\phi_{m'j^\pm}) \delta(t - t_{m'}). \quad (5.1)$$

It will be convenient to choose the times $t_m = m\Delta t$ and the space points $z_j = j\Delta z$ to correspond to the points in a two-dimensional space-time grid to be used in the numerical solution of Eqs. (3.5) (see Fig. 1).

In order to determine the normalization constant A_s , let us apply Eqs. (3.5) to the case of an infinite homogeneous medium near thermodynamic equilibrium. The solution of Eq. (3.5c) for $p=0$ and S^+ as given in Eq. (5.1) is

$$\rho_0^+ = -\frac{1}{2}n\sigma_0\mathcal{E}^+ + A_s \sum_{m'} u(t - t_{m'}) \exp[i\phi_{m'} - T_2^{-1}(t - t_{m'})], \quad (5.2)$$

where spatial variations have been neglected. The first term on the right-hand side of Eq. (5.2) comes from a rate-equation approximation, which is valid near equilibrium; the second term is exact. Also, the phase variable in the second term has been abbreviated to $\phi_{m'}$. The function $u(t)$ represents a unit step function which differs from 0 for positive arguments. After substitution of expression (5.2) into Eq. (3.5a) and the neglect of the spatial derivative, (3.5a) becomes

$$\frac{d\mathcal{E}^+}{dt} + \frac{c}{2\eta}(N_1 - N_2)\sigma_0\mathcal{E}^+ = \frac{c}{\eta}A_s \sum_{m'} u(t - t_{m'}) \times \exp[i\phi_{m'} - T_2^{-1}(t - t_{m'})]. \quad (5.3)$$

The population difference $n = N_2 - N_1$ has been written explicitly to emphasize the connection between the equation which arises from (5.3) and the usual Einstein equation for radiative equilibrium. Equation (5.3) has the form of the Langevin equation

$$\frac{d\mathcal{E}^+}{dt} + \beta\mathcal{E}^+ = F(t), \quad (5.4)$$

with $\beta = (c/2\eta)(N_1 - N_2)\sigma_0$. The solution to Eq. (5.4) is

$$\mathcal{E}^+(t) = \mathcal{E}^+(0)e^{-\beta t} + \int_0^t e^{-\beta(t-t')} F(t') dt'. \quad (5.5)$$

An equation for $|\mathcal{E}^+|^2$ can be derived by multiplying Eq. (5.4) by \mathcal{E}^{+*} and adding the complex conjugate

⁴⁸ Numerous authors have treated laser noise analytically or semianalytically using the Langevin method. For this purpose it is usually unnecessary to specify the specific noise model as is done here. See, for example, H. Haken, *Z. Physik* **190**, 327 (1966).

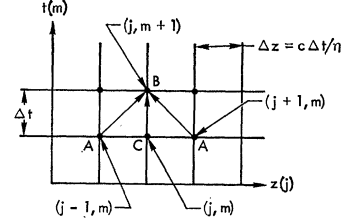


FIG. 1. Finite-difference grid for numerical solution of Eqs. (6.1). Arrows indicate integration paths used in reducing differential equations to finite difference equations. Paths AB are used for Eqs. (6.1a) and (6.1b) and path CB for the remaining equations. Each grid point in the amplifying region is supplied with a δ -function source, which creates a fluctuating contribution to the dipole moment.

equation. The result is

$$\frac{d|\mathcal{E}^+|^2}{dt} + 2\beta|\mathcal{E}^+|^2 = \mathcal{E}^{+*}F(t) + \text{c.c.} \quad (5.6)$$

To derive the Einstein equation one takes an ensemble average over Eq. (5.6), obtaining

$$\frac{d}{dt} \langle |\mathcal{E}^+|^2 \rangle + 2\beta \langle |\mathcal{E}^+|^2 \rangle = \langle \mathcal{E}^{+*}F(t) \rangle + \text{c.c.}, \quad (5.7)$$

where use has been made of the commutability of the derivative and ensemble averaging operations. To calculate the average $\langle \mathcal{E}^{+*}F(t) \rangle$, we use expression (5.5) for $\mathcal{E}^+(t)$ in the limit of large t , obtaining

$$\langle \mathcal{E}^{+*}F(t) \rangle = \int_0^\infty e^{-s\beta} \langle F^*(t-s)F(t) \rangle ds. \quad (5.8)$$

The correlation function $\langle F^*(t-s)F(t) \rangle$ is readily evaluated for the function appearing on the right-hand side of (5.3). For t and s taken at the sampling times t_m , the correlation function is independent of time and is given by

$$\begin{aligned} \langle F^*(t-s)F(t) \rangle &= \left[\left(\frac{c}{\eta} \right) A_s \right]^2 \\ &\times \exp(-T_2^{-1}s) \sum_{n=0}^\infty \exp(-2T_2^{-1}n\Delta t) \\ &= \frac{[(c/\eta)A_s]^2 \exp(-T_2^{-1}s)}{1 - \exp(-2T_2^{-1}\Delta t)}. \end{aligned} \quad (5.9)$$

Substitution of expression (5.9) into Eq. (5.8) allows us to express Eq. (5.7) in the form

$$\begin{aligned} \frac{d}{dt} \langle |\mathcal{E}^+|^2 \rangle + \frac{c}{\eta} \sigma_0 (N_1 - N_2) \langle |\mathcal{E}^+|^2 \rangle \\ &= \frac{2[(c/\eta)A_s]^2}{[1 - \exp(-2T_2^{-1}\Delta t)](\beta + T_2^{-1})} \\ &\approx \frac{2(c/\eta)^2 T_2 A_s^2}{[1 - \exp(-2T_2^{-1}\Delta t)]}, \end{aligned} \quad (5.10)$$

where the approximate expression holds if $\beta \ll T_2^{-1}$, which is ordinarily the case.

Equation (5.10) thus has the form of the Einstein equation, where the right-hand side can be expressed as $2(c/\eta)^2 T_2 A_s^2 / [1 - \exp(-2T_2^{-1}\Delta t)] = cN_2 f / \tau_s \eta$. (5.11)

Here, τ_s is the spontaneous emission lifetime and f is the fraction of the total solid angle subtended by \mathcal{E}^+ . Solving for A_s^2 gives

$$A_s^2 = [1 - \exp(-2T_2^{-1}\Delta t)] N_2 f \eta / 2cT_2 \tau_s. \quad (5.12)$$

Equations (5.1) and (5.12) completely specify the spontaneous emission model.⁴⁹

The sampling interval Δt is determined by the requirement that sampling times should be frequent enough to provide an accurate description of the correlation function (5.9). Thus Δt should be somewhat smaller than T_2 . We can also arrive at this criterion with the help of sampling theory. With a sampling interval Δt we can expect to reproduce a spectrum of width⁵⁰

$$\Delta\nu = 1/2\Delta t. \quad (5.13)$$

For the spectrum of (5.9), which is Lorentz with full width $\Delta\nu = (\pi T_2)^{-1}$, (5.13) becomes

$$\Delta t = \frac{1}{2}\pi T_2. \quad (5.14)$$

To accurately define the spectrum of (5.9) we therefore need a value of Δt somewhat smaller than the value in (5.14). Furthermore, the accurate reduction of the differential equations (3.5c) and (3.5d) to difference equations requires the fulfillment of the same criterion on Δt because of the presence of the relaxation time T_2 in the former equations. The calculations to be described in Sec. VII have been carried out for values $\Delta t = \frac{1}{4}T_2$ and $\Delta t = \frac{1}{3}T_2$.

VI. FINITE DIFFERENCE APPROXIMATIONS TO TW EQUATIONS DERIVED FROM FOURIER SERIES

The numerical solution of a set of ordinary differential equations with given initial conditions can be accomplished by a straightforward application of some scheme of wide applicability such as the Runge-Kutta method. But the reduction of a system of partial differential equations to finite difference form suitable for

⁴⁹ A Fourier series representation of spontaneous emission has also been tried in Ref. 40. There are, however, several defects to this method. First of all, it is time consuming if one wishes to reproduce a wide spectrum; second, it introduces a discrete spectrum where a continuous spectrum really applies. One is then hard put to decide whether the effects observed are influenced by the assumed mode structure of the noise source. It is preferable to use a noise source with a continuous spectrum and let the laser determine its own mode structure.

⁵⁰ Strictly speaking, to reconstruct the entire function from the sampled data one needs to employ an interpolation formula $f(t) = \sum_n f_n g(t - m\Delta t)$ where $g(t)$ is a sampling function. See, for example, L. Brillouin, *Science and Information Theory* (Academic Press Inc., New York, 1956), p. 93. In deriving difference equations we have employed only linear interpolations.

computation must be tailored to the idiosyncrasies of the system at hand. Whereas a Runge-Kutta scheme can be counted on to give fourth-order accuracy, special pains are usually required to achieve second-order accuracy in the solution of partial differential equations.⁵¹ Whenever many integration cycles are required, as in the present application, where as many as 90 000 cycles may be required, it is essential to employ a second-order scheme, both to preserve accuracy⁵² and to minimize computing time.

For convenience, we repeat here the complete set of equations obtained from (3.5) in the case of $p_{\max} = 1$:

$$\frac{\eta}{c} \frac{\partial \mathcal{E}^+}{\partial t} + \frac{\partial \mathcal{E}^+}{\partial z} = -\rho_0^+, \quad (6.1a)$$

$$\frac{\eta}{c} \frac{\partial \mathcal{E}^-}{\partial t} - \frac{\partial \mathcal{E}^-}{\partial z} = -\rho_0^-, \quad (6.1b)$$

$$\frac{\partial \rho_0^+}{\partial t} + T_2^{-1} \rho_0^+ = -\frac{1}{2} T_2^{-1} \sigma_0 (\bar{n} \mathcal{E}^+ + n_1 \mathcal{E}^-) + S^+, \quad (6.1c)$$

$$\frac{\partial \rho_0^-}{\partial t} + T_2^{-1} \rho_0^- = -\frac{1}{2} T_2^{-1} \sigma_0 (\bar{n} \mathcal{E}^- + n_1^* \mathcal{E}^+) + S^-, \quad (6.1d)$$

$$\frac{\partial \rho_1^+}{\partial t} + T_2^{-1} \rho_1^+ = -\frac{1}{2} T_2^{-1} \sigma_0 n_1 \mathcal{E}^+, \quad (6.1e)$$

$$\frac{\partial \rho_1^-}{\partial t} + T_2^{-1} \rho_1^- = -\frac{1}{2} T_2^{-1} \sigma_0 n_1^* \mathcal{E}^-, \quad (6.1f)$$

$$\frac{\partial \bar{n}}{\partial t} + T_1^{-1} (\bar{n} - n^0) = 4(\mathcal{E}^- \rho_0^+ + \mathcal{E}^+ \rho_0^- + \text{c.c.}), \quad (6.1g)$$

$$\frac{\partial n_1}{\partial t} + T_1^{-1} n_1 = 4(\mathcal{E}^- \rho_0^+ + \mathcal{E}^+ \rho_1^+ + \mathcal{E}^+ \rho_0^- + \mathcal{E}^- \rho_1^*). \quad (6.1h)$$

A useful strategy to follow in deriving both stable and accurate difference schemes from systems of equations such as (6.1) is to express the differentiated variable appearing on the left-hand side of a given equation in terms of an integral over the right-hand side. The integral can then be approximated numerically. Furthermore, integrals over the singular source terms in Eqs. (6.1c) and (6.1d) can be handled *exactly*.

In Eqs. (6.1), the following two types of equations are represented:

$$\frac{dx}{dt} + T^{-1}x = f, \quad (6.2a)$$

⁵¹ “ N th-order accuracy” implies that the truncation error in the dependent variables is of order $N+1$ in the increments of one or more independent variables, while the truncation error in first derivatives is N th order in the same increments.

⁵² The calculations to be described were performed on a CDC 6600 computer which carries the equivalent of 14 significant decimal digits.

$$\frac{\eta}{c} \frac{\partial y}{\partial t} \pm \frac{\partial y}{\partial z} = g. \quad (6.2b)$$

If Eq. (6.2a) is integrated from $t_m = m\Delta t$ to t_{m+1} the result can be expressed as

$$x_j^{m+1} = x_j^m e^{-\Delta t/T} + \int_{t_m}^{t_{m+1}} e^{-(t-t')/T} f(t') dt', \quad (6.3)$$

where $x_j^m = x(j\Delta z, m\Delta t)$. If $f(t')$ is assumed to vary linearly in time between t_m and t_{m+1} , the integral can be evaluated explicitly with the result

$$x_j^{m+1} = Cx_j^m + Af_j^m + Bf_j^{m+1} + O((\Delta t)^3), \quad (6.4)$$

where $f_j^m = f(j\Delta z, m\Delta t)$ and

$$\begin{aligned} C &= e^{-\Delta t/T}, \\ A &= T[(T/\Delta t)(1 - e^{-\Delta t/T}) - e^{-\Delta t/T}], \\ B &= T[1 - (T/\Delta t)(1 - e^{-\Delta t/T})]. \end{aligned} \quad (6.5)$$

Equation (6.4) is the basis for the difference equations which are used to approximate Eqs. (6.1c)–(6.1h). In addition to the fact that the difference scheme (6.4) is of second order, a further advantage is that as $T/\Delta t$ is allowed to approach 0, x_j^{m+1} approaches Tf_j^{m+1} . This means that in the limit of large time increments, the numerical solutions to Eqs. (6.1c)–(6.1f) can approach their “rate-equation” form.

The total derivative which appears on the left-hand side of Eq. (6.2b) can be expressed in terms of a directional derivative in the z, t plane. The direction is that of the characteristic which has direction cosines

$$\begin{aligned} l_z &= \pm \frac{1}{[(\eta/c)^2 + 1]^{1/2}}, \\ l_t &= \frac{\eta/c}{[(\eta/c)^2 + 1]^{1/2}}. \end{aligned} \quad (6.6)$$

In terms of this directional derivative, Eq. (6.2b) becomes

$$D \frac{dy}{ds} = g, \quad (6.7)$$

where

$$D = [(\eta/c)^2 + 1]^{1/2}. \quad (6.8)$$

Assuming that $c\Delta t/\eta = \Delta z$ and integrating Eq. (6.6) from $A \equiv (z_{j\mp 1}, t_m)$ to $B \equiv (z_j, t_{m+1})$ (see Fig. 1), one obtains

$$y_j^{n+1} - y_{j\mp 1}^n = D^{-1} \int_A^B g ds. \quad (6.9)$$

If now it is assumed that g varies linearly along the characteristic between A and B , Eq. (6.9) becomes

$$y_j^{n+1} - y_{j\mp 1}^n = \frac{1}{2} \Delta z (g_j^{n+1} + g_{j\mp 1}^n) + O((\Delta z)^3). \quad (6.10)$$

Equation (6.10) forms the basis for the finite difference equations which replace Eqs. (6.1a) and (6.1b).

When Eqs. (6.1) have been differenced according to the schemes represented in Eqs. (6.4) and (6.10), the result is eight implicit difference equations, i.e., which contain the updated variables on both sides of the equal signs. It is obviously far simpler to work with complex variables than it is to introduce real amplitudes and phases, which would require further complicated algebraic reduction. In the former case one can simply make use of complex arithmetic operations which are available in most computer compilers. To illustrate the method of solution, we write in detail the difference equations which represent Eqs. (6.1a)–(6.1h). Using Eqs. (6.4) and (6.10), one obtains

$$\mathcal{E}_j^{+m+1} = \mathcal{E}_{j-1}^{+m} - \frac{1}{2} \Delta z (\rho_{0j}^{+m+1} + \rho_{0j-1}^{+m}), \quad (6.11a)$$

$$\mathcal{E}_j^{-m+1} = \mathcal{E}_{j+1}^{-m} - \frac{1}{2} \Delta z (\rho_{0j}^{-m+1} + \rho_{0j+1}^{-m}), \quad (6.11b)$$

$$\begin{aligned} \rho_{0j}^{+m+1} &= C_2 \rho_{0j}^{+m} - \frac{1}{2} T_2^{-1} \sigma_0 A_2 (\bar{n}_j^m \mathcal{E}_j^{+m} + n_{1j}^m \mathcal{E}_j^{-m}) \\ &\quad - \frac{1}{2} T_2^{-1} \sigma_0 B_2 (\star \bar{n}_j^{m+1} \mathcal{E}_j^{+m+1} + \star n_{1j}^{m+1} \mathcal{E}_j^{-m+1}) \\ &\quad + A_s \exp(i\phi_{m+1,j}^+), \end{aligned} \quad (6.11c)$$

$$\begin{aligned} \rho_{0j}^{-m+1} &= C_2 \rho_{0j}^{-m} - \frac{1}{2} T_2^{-1} \sigma_0 A_s (\bar{n}_j^m \mathcal{E}_j^{-m} + n_{1j}^m \mathcal{E}_j^{+m}) \\ &\quad - \frac{1}{2} T_2^{-1} \sigma_0 B_2 (\star \bar{n}_j^{m+1} \mathcal{E}_j^{-m+1} + \star n_{1j}^{m+1} \mathcal{E}_j^{+m+1}) \\ &\quad + A_s \exp(i\phi_{m+1,j}^-), \end{aligned} \quad (6.11d)$$

$$\begin{aligned} \rho_{1j}^{+m+1} &= C_2 \rho_{1j}^{+m} - \frac{1}{2} T_2^{-1} \sigma_0 (A_2 n_{1j}^m \mathcal{E}_j^{+m} \\ &\quad + B_2 n_{1j}^{m+1} \mathcal{E}_j^{+m+1}), \end{aligned} \quad (6.11e)$$

$$\begin{aligned} \rho_{1j}^{-m+1} &= C_2 \rho_{1j}^{-m} - \frac{1}{2} T_2^{-1} \sigma_0 (A_2 n_{1j}^m \mathcal{E}_j^{-m} \\ &\quad + B_2 n_{1j}^{m+1} \mathcal{E}_j^{-m+1}), \end{aligned} \quad (6.11f)$$

$$\begin{aligned} \bar{n}_j^{m+1} &= C_1 \bar{n}_j^m + A_1 [T_1^{-1} n^0 \\ &\quad + 4(\mathcal{E}_j^{-*m} \rho_{0j}^{-m} + \mathcal{E}_j^{+*m} \rho_{0j}^{+m} + \text{c.c.})] \\ &\quad + B_1 [T_1^{-1} n^0 + 4(\mathcal{E}_j^{-*m+1} \rho_{0j}^{-m+1} \\ &\quad + \mathcal{E}_j^{+*m+1} \rho_{0j}^{+m+1} + \text{c.c.})], \end{aligned} \quad (6.11g)$$

$$\begin{aligned} n_{1j}^{m+1} &= C_1 n_{1j}^m + 4A_1 (\mathcal{E}_j^{-*m+1} \rho_{0j}^{+m+1} + \mathcal{E}_j^{+*m+1} \rho_{1j}^{+m+1}) \\ &\quad + \mathcal{E}_j^{+m+1} \rho_{0j}^{-*m+1} + \mathcal{E}_j^{-m+1} \rho_{1j}^{-*m+1}) \\ &\quad + 4B_1 (\mathcal{E}_j^{-*m} \rho_{0j}^{+m} + \mathcal{E}_j^{+*m} \rho_{0j}^m \\ &\quad + \mathcal{E}_j^{+m} \rho_{0j}^{-*m} + \mathcal{E}_j^{-m} \rho_{1j}^{-*m}). \end{aligned} \quad (6.11h)$$

In writing Eqs. (6.11c) and (6.11d) we have chosen to replace \bar{n}_j^{m+1} and n_{1j}^{m+1} by their linearly extrapolated values from the two previous integration cycle times. This is permissible because \bar{n} and n_1 vary much more slowly than \mathcal{E}^+ , \mathcal{E}^- , ρ_0^+ , and ρ_0^- . The prefixed \star in Eqs. (6.11c) and (6.11d) signifies forward extrapolation, and the constants C_1 , A_1 , B_1 , and C_2 , A_2 , B_2 are obtained from the appropriate one of Eqs. (6.5) by substitution of T_1 and T_2 for T . Spontaneous emission contributes complex constants with constant amplitudes but random phases on the right-hand side of Eqs. (6.11c) and (6.11d). Expressions (6.11c) and (6.11d) for ρ_{0j}^{+m+1} and ρ_{0j}^{-m+1} , after substitution into Eqs. (6.11a) and (6.11b), lead to two equations of the form

$$\alpha_1 \mathcal{E}_j^{+m+1} + \beta_1 \mathcal{E}_j^{-m+1} = \Gamma_1, \quad (6.12a)$$

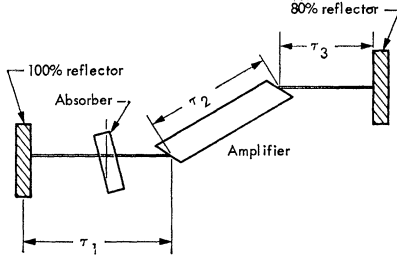


FIG. 2. Laser cavity geometry used in calculations.

$$\alpha_2 \mathcal{E}_j^{+m+1} + \beta_2 \mathcal{E}_j^{-m+1} = \Gamma_2, \quad (6.12b)$$

which are solved simultaneously for \mathcal{E}_j^{+m+1} and \mathcal{E}_j^{-m+1} .

The next steps in order are the simultaneous determinations of \bar{n}_j^{m+1} and n_{1j}^{m+1} from Eqs. (6.11g) and (6.11h). In order to do this, ρ_{0j}^{+m+1} , ρ_{0j}^{-m+1} , ρ_{1j}^{+m+1} , ρ_{1j}^{-m+1} are first eliminated from the latter difference equations by means of expressions (6.11c)–(6.11f). In the resulting forms of (6.11g) and (6.11h), all stars are dropped from \bar{n}_j^{m+1} and n_{1j}^{m+1} . The cycle is completed by solving (6.11c), (6.11d), (6.11g), and (6.11h) without stars for ρ_{0j}^{+m+1} , ρ_{0j}^{-m+1} , ρ_{1j}^{+m+1} , and ρ_{1j}^{-m+1} . Separate regions with different parameters must, of course, be established for the absorbing and amplifying media in the cavity. In those parts of the laser cavity where air gaps exist, the material variables are disregarded and the “streaming” of radiation is described exactly by means of Eqs. (6.11a) and (6.11b) without the parenthesis terms. Finally, the boundary conditions at the cavity ends are taken to be the reflection conditions

$$\begin{aligned} \mathcal{E}_0^{+m+1} &= -r_1 \mathcal{E}_0^{-m+1}, \\ \mathcal{E}_J^{-m+1} &= -r_2 \mathcal{E}_J^{+m+1}, \end{aligned} \quad (6.13)$$

where mirrors having amplitude reflection coefficients r_1 and r_2 are assumed to be at positions $z=0$ and $z=J\Delta z$, J being the number of zones in the cavity. The cycle may be repeated with the improved updated values of \bar{n}_j^{m+1} and n_{1j}^{m+1} in Eqs. (6.11c) and (6.11d), but this step usually proves unnecessary.

VII. NUMERICAL EXAMPLES

The geometry which is treated is that of a typical Fabry-Perot cavity shown in Fig. 2. For the purposes of numerical integration, the optical path between the two mirrors is subdivided into zones which are traversed by light in the same time Δt , regardless of medium. The length of a given zone must then be $\Delta z = c\Delta t/\eta$ where η is the medium refractive index. In all cases considered, the respective intensity-reflection coefficients of the two mirrors are 100 and 80%, the optical round-trip time between mirrors is 3.68 nsec, and the amplifying section is assumed to be a 7.5-cm ruby with $\sigma_0 = 2.5 \times 10^{-20}$ cm, $T_1 = 3 \times 10^{-3}$ sec, and $N = 1.62 \times 10^9/\text{c.c.}$ In addition, the optical travel times indicated in Fig. 2 are $\tau_1 = 0.91$ nsec, $\tau_2 = 0.44$ nsec, $\tau_3 = 0.49$ nsec.

For ruby at room temperature, $T_2 \approx 1.0$ psec. The appropriate T_2 for typical dyes is not known, but it should be at least this small. Unfortunately, it turns out to be impractical to solve the system (6.1) numerically for cavities of experimental dimensions if values of T_2 of the above magnitude are used. In the calculations which are described here, T_2 is restricted to the range 10–20 psec. Thus, we do not seek quantitative agreement between calculation and experiment in these calculations, but we can expect to gain a qualitative but detailed insight into certain multimode effects, which has not been hitherto attainable by other methods.

A. Operation of Q-Switched Laser with Absorber in Cavity

We turn our attention first to the case in which the laser is switched by means of a saturable absorber in the cavity. We assume that the absorbing medium is directly adjacent to the 100% mirror and has a 1.0 cm thickness. We also assume that for the absorber $\sigma_0 = 8.0 \times 10^{-16}$ cm², corresponding to cryptocyanine, and $N = 1.0 \times 10^{15}$ cm⁻³. The resulting single-pass low-power transmission is 55%. For convenience, we take the index of refraction to be 1.76 in both the absorber and the amplifying media. For the absorber we take $T_1 = 80$ psec,⁵³ and for both the absorber and the amplifier we take $T_2 = 20$ psec. For the dimensions of the cavity under consideration there are thus a total of 60 modes within the full width of the Lorentz line, compared to the 1200 modes which would be present for the experimental fluorescence width. The cavity is divided into 376 spatial zones defined by 377 grid points. The amplifying medium contains 90 zones and the absorbing medium 12 zones. The time increment Δt is taken to be 4.9 psec,⁵⁴ and for the purpose of determining the spontaneous emission constant A_s it is assumed that the laser beam angle is 10^{-3} rad.

The evolution of a Q-switched mode-locked laser pulse from noise over round-trip time periods is exhibited in Figs. 3(a)–3(h), which have been plotted by the computer. The growth in intensity is initiated by setting in the amplifying medium $n_1(z) = 0$ and $\bar{n}(z)$ equal to its threshold value plus 3.8%, which happens to be 33.6% of the active atom density. Obviously, the experimental situation would differ somewhat in that $\bar{n}(z)$ would be brought to its threshold value and above continuously and over a period of time which is long compared to the time represented in our calculations.

⁵³ Decay lifetimes as short as 6 psec have been reported for Eastman dye 9860, used to switch Nd-glass lasers, by R. I. Scarlet, J. F. Figueira, and H. Mahr, Appl. Phys. Letters 13, 71 (1968). This author is not aware of similar measurements applying to dyes used with ruby. The value of T_1 selected here was chosen simply to be several times as large as T_2 .

⁵⁴ According to relation (5.13), we should have contributions from 376 modes to the numerically generated spectrum, although the contributions from the highest-order modes may not be handled too accurately.

However, computation time considerations dictate the method of starting used here.

The pulse evolution can be divided into three stages. In the initial stage [Figs. 3(a)–3(d)], the intensity is low enough that both the amplification and absorption processes can be considered to be linear. The intensity pattern is that of amplified spontaneous emission and obviously represents Gaussian random noise. Initially the intensity output is aperiodic, but as the radiation is amplified above noise background there are quasi-periodic similarities between the emissions over different round trips. Since the laser exhibits net amplification,

the radiation undergoes spectral narrowing. This effect is exhibited in the time domain as a smoothing and broadening of pulses existing in the round-trip patterns.

In the second phase of pulse evolution [Figs. 3(d)–3(g)], the absorption is nonlinear, but the amplification is linear. This phase ends when the absorbing transition is completely saturated. As the result of nonlinear absorption, two effects take place. First, there is a selective emphasis of certain of the pulses already present. Since the processes involved are frequency-dependent, the selection may not always be on the basis of height alone. For ideal mode locking, the number of

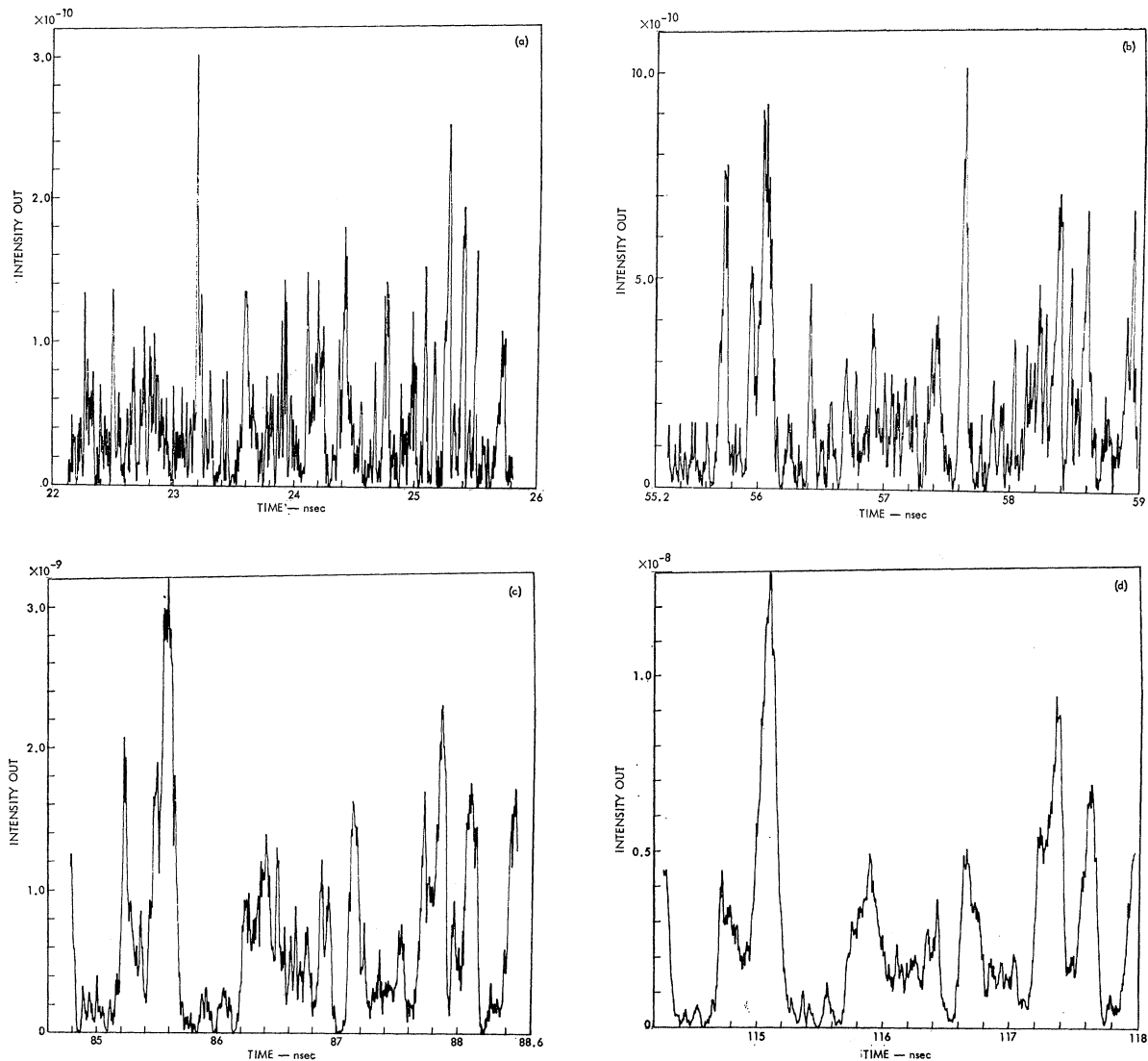


FIG. 3. Evolution of a Q-switched mode-locked pulse train from spontaneous emission noise for absorber next to mirror. Each picture represents output intensity over a single round-trip period of 3.68 nsec. Intensity is measured in units of 1.62×10^{19} photons/nsec cm^2 or 4.64 GW/cm^2 in these and all subsequent figures. (a)–(d) Low-power emission. Both amplification and absorption are linear. Slight excess of gain leads to spectral narrowing which shows up in the time domain as a smoothing and broadening of pulse structure. (e)–(g) Intermediate power. Nonlinear action of absorber broadens spectrum and selectively emphasizes one pulse. Amplification is linear, however, and this tends to counteract spectral broadening by absorber. (h) High power. Pulse structure at maximum intensity. Background pulses have been almost completely suppressed. However, pulse narrowing in time due to nonlinear gain is minimal.

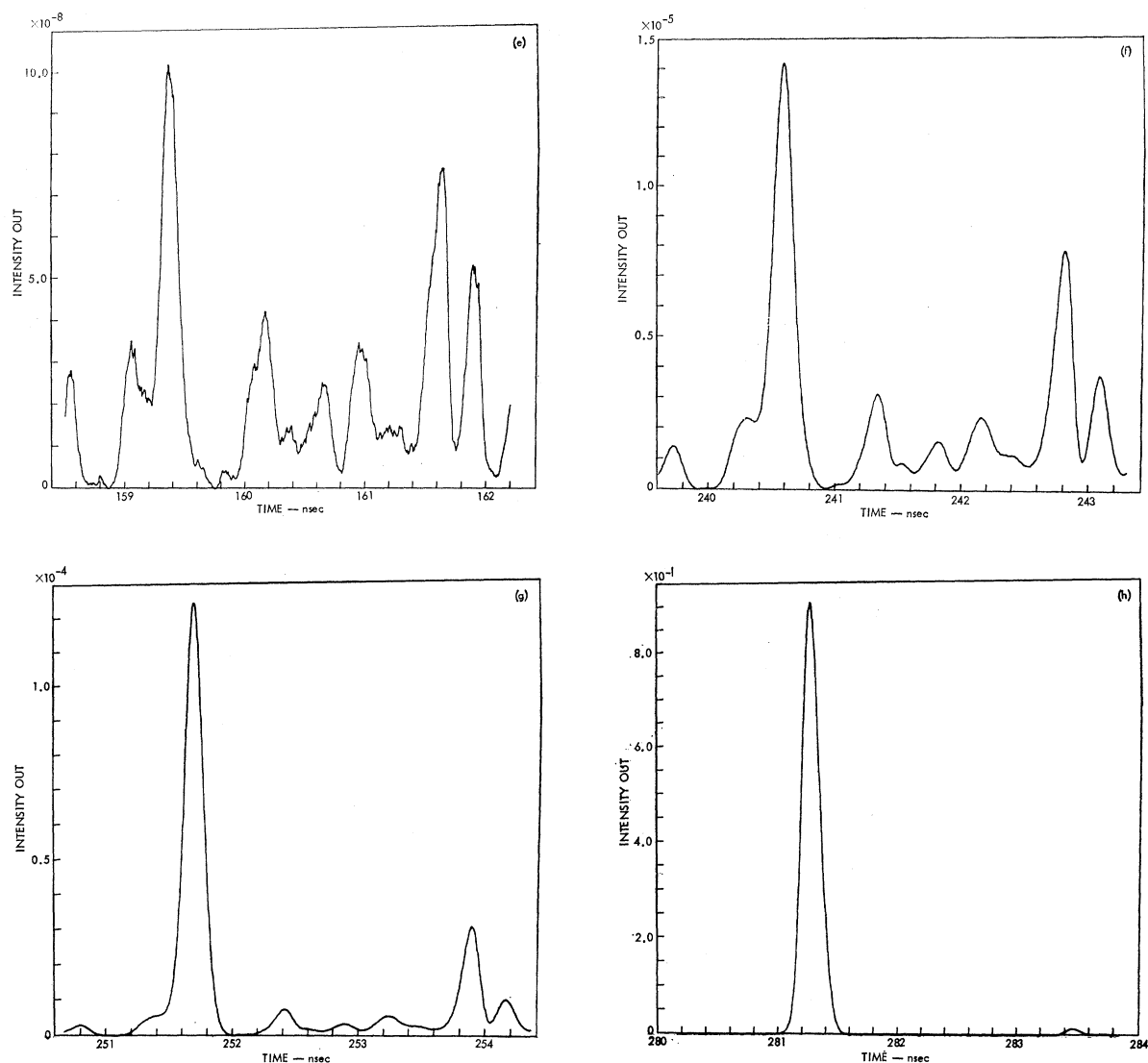


FIG. 3. (continued)

pulses per round trip should be narrowed down to one. In the case under consideration here the elimination of background pulses is almost complete, as is seen in Fig. 3(h) which represents the pulse of maximum intensity in the entire train. The second effect of nonlinear absorption is spectral broadening which tends to narrow the existing pulses in time. This effect, however, is partly counteracted by the tendency of the linearly amplifying region to narrow the spectrum.

The final phase of the pulse evolution occurs when the intensity is sufficiently high for complete saturation of the absorber transition to take place and for the amplification to be nonlinear. It would be expected that the nonlinear amplification would further broaden the spectrum and narrow the temporal width of the pulse. However, this does not happen, as can be seen by com-

paring Figs. 3(g) and 3(h). One would certainly expect nonlinear pulse narrowing in time to take place after the passage of radiation through a sufficiently long path in an amplifying medium. When the path is folded back and forth upon itself as it is within a laser cavity, however, the nonlinear pulse-shaping capability can be very much reduced if the pump cannot restore the inversion lost during each pass before the reflected pulse reenters the amplifying medium. This is the situation encountered with solid-state lasers.

The minimum pulse width which is exhibited by the pulse in Fig. 3(h) is 145 psec. This is 2.4 times the reciprocal of the fluorescent bandwidth $\Delta\nu^{-1}$ which is generally regarded as the lower bound to the duration of mode-locked pulses and which also represents a lower limit for the Q -switched mode-locked pulses which have

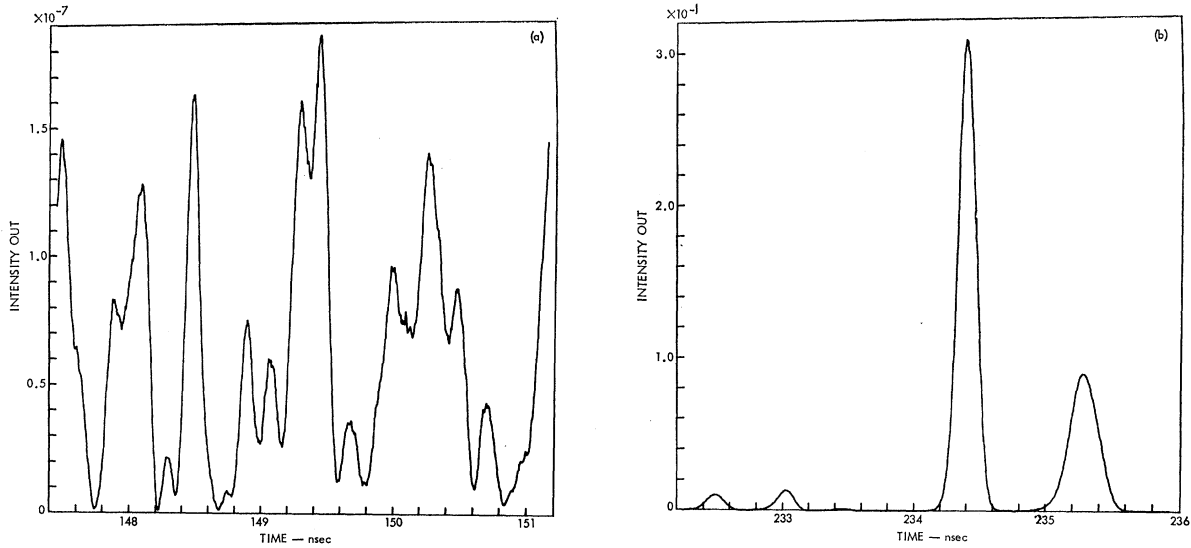


FIG. 4. Evolution of mode-locked pulse train from noise. Same conditions as in Fig. 3, except that spontaneous emission is determined by different random phases. (a) Intermediate power. Output pattern at beginning of nonlinear action by absorber. (b) Fully evolved pulse pattern at high power. Suppression of background pulses is incomplete. This and Fig. 3 suggest that a statistical element is involved in the production of well-defined mode-locked pulses.

been observed experimentally.^{11-14,55,56} It has been established theoretically that nonlinear amplification can lead to pulses which are shorter than T_2 when high enough intensities are available to create a sufficiently strong nonlinearity.^{27,31,35} Conditions for such pulse shortening are extremely difficult to achieve experimentally and are apparently not realized in the generation of short pulses by solid-state laser oscillators. Since the strength of the nonlinear interaction between the radiation and the matter is determined by the constant $\bar{\mu}$ rather than by σ_0 , the problem of Figs. 3(a)-3(h) was rerun with a value of σ_0 twenty times greater than the room-temperature value previously assumed to determine whether the correct value of $\bar{\mu}$ for ruby would lead to any differences. This case would correspond to ruby at a temperature of 110°K. This change produced no difference in the final pulse widths. The only difference was that the peak intensity was lower than in the previous case by a factor of 20.

In order to test the effect on the final pulse structure of the initial noise pattern, the problem was rerun with the room temperature σ_0 and a different set of random phases in the spontaneous emission sources. The intensity pattern over one round trip is shown in Fig. 4(a) at a power where the maximum absorber population difference is -98%. The pulse pattern over one round trip close to peak power, displayed in Fig. 4(b), clearly shows that the elimination of background pulses is incomplete. These results agree with experimental findings that there is a statistical factor in the produc-

tion of well-defined mode-locked pulses.⁵⁷ To determine the effect of operating the laser near threshold on pulse formation, this problem was rerun from time $t=148.0$ nsec with $\bar{n}(z)$ in the amplifying medium lowered to the threshold value. The main effect of operating near the threshold is to lengthen the time during which nonlinear absorption takes place. The result of this calculation was that the background pulses in Fig. 4(b) were completely eliminated, and the final pulse width was reduced to $2\Delta\nu^{-1}$. This result is in agreement with experimental findings that statistics are better for the production of well-defined mode-locked pulses when the laser is operated near threshold than when it is operated well above.⁵⁷

The effect of placing the center of the absorber at a point which is located one-third the distance between the two mirrors is shown in Figs. 5(a) and 5(b). The final output pattern in Fig. 5(b) indicates the presence of three pulses per round trip spaced so that two can always cross at the absorber.⁵⁸ This example clearly indicates how a selective emphasis of random noise beats through nonlinear absorption brings about mode locking in passively switched lasers.^{38,39}

It has already been noted that an appreciable change in pulse width does not take place during nonlinear amplification. An experimental determination of the time duration of mode-locked pulses from Nd-glass lasers, on the other hand, has indicated that during nonlinear amplification pulse durations increase with

⁵⁷ G. Kachen (private communication).

⁵⁵ S. L. Shapiro and M. A. Duguay, Phys. Letters 8A, 698 (1969).

⁵⁶ G. Kachen, Appl. Phys. Letters 13, 229 (1968).

⁵⁸ Such patterns for intermediate positioning of the absorber have been found experimentally by A. Schmackpfeffer and H. Weber, Phys. Letters 24A, 190 (1967); R. Harrach and G. Kachen, J. Appl. Phys. 39, 3482 (1968).

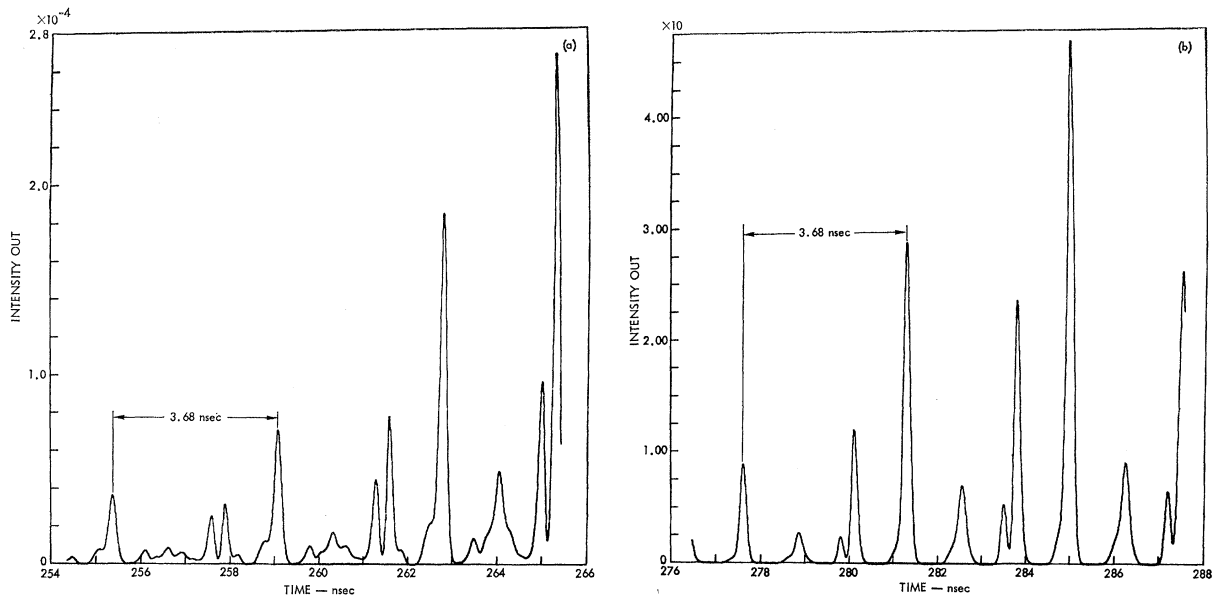


FIG. 5. Evolution of mode-locked pulse train from noise when absorber is placed one-third the distance between mirrors. Output is shown over three round-trip periods. Pulse pattern is such that two pulses always cross simultaneously at absorber, thus enhancing nonlinear action. (a) Intermediate power. Shaping of noise pattern through nonlinear action of the filter. (b) High power. Pulse pattern has evolved into three prominent pulses per round trip.

power.¹² A similar effect has not been reported for ruby. It has also been reported that pulses from Nd-glass lasers are frequency-swept or "chirped,"²⁴⁵ presumably as the result of dispersion, either linear or nonlinear,^{36,59} in one or both of the host media containing the absorbing and amplifying atoms. The calculations under dis-

cussion here show negligible frequency sweeps of the order of 10^9 rad/sec/pulse.

B. Laser Q-Switched by Active Means

We turn our attention next to the operation of a Q-switched laser with no absorbing medium in the cavity. The cavity and starting conditions are the same

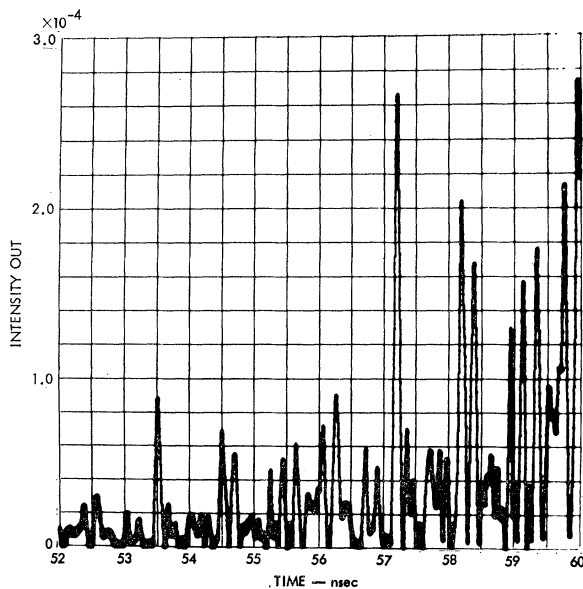


FIG. 6. Intensity pattern for Q-switched laser switched by mechanical or electro-optic means. Power is roughly three orders of magnitude below peak power, and amplification is still linear.

⁵⁹ R. A. Fisher, P. L. Kelley, and T. K. Gustafson, *Appl. Phys. Letters* 14, 140 (1969).

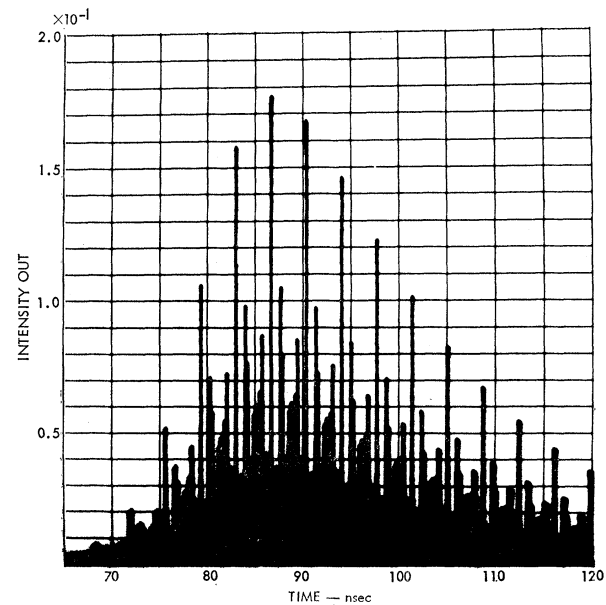


FIG. 7. Detailed shape of giant pulse. Fluctuations in intensity are caused by spontaneous emission source rather than by coherent dipole effects.

as in the previous case, with the following exceptions. The initial value of $\bar{n}(z)$ is taken to be 23% of the active atom density and T_2 has been lowered to 10 psec (120 modes in the spectrum at half-maximum). Also, Δt has been reduced to 3.27 psec and the optical path between mirrors has been divided into 564 zones. A detailed history of the pulse-pattern evolution like that in Figs. 3 will not be included here, since much of it will be similar to the first phase of the mode-locked pulse evolution. The sharp patterns which are present initially are smoothed as the result of spectral narrowing by amplification. There is, however, no pulse-selection mechanism, and the pulses which are present, say, three orders of magnitude below peak intensity (Fig. 6), are present throughout nonlinear amplification. Nonlinear amplification, however, causes a slight distortion in the round-trip pulse pattern. The complete giant pulse envelope is shown in Fig. 7 and the pulse pattern emitted over one round-trip time when maximum intensity occurs is shown in Fig. 8.⁶⁰ The pulses in this pattern are typically $\approx 10T_2$ in duration.

In order to test the laser output depicted in Figs. 7 and 8 for its similarity to Gaussian noise, the normalized two-photon fluorescence pattern has been calculated for the entire emission history. The integrated fluorescence intensity $f(\tau)$ normalized to its value for $\tau \ll T$ is given by¹⁶

$$f(\tau) = 1 + 2G(\tau), \quad (7.1a)$$

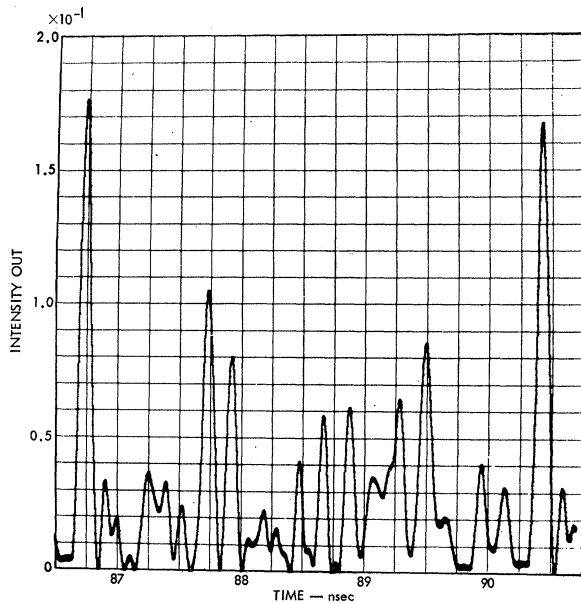


FIG. 8. Pulse structure detail over single round-trip period at maximum power.

⁶⁰ There is no chance that the fluctuating emission pattern is due to a "ringing" of the electric field caused by changes in sign of the population difference, such as is reported in Refs. 28 and 30, because the population difference variable $\bar{n}(z)$ approaches 0 monotonically.

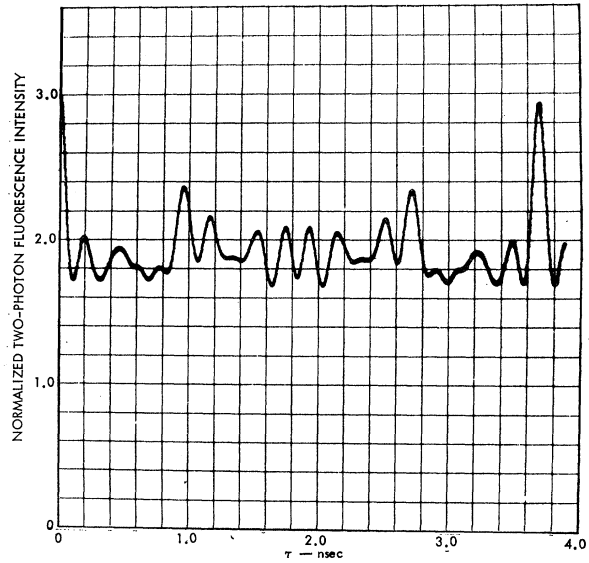


FIG. 9. Normalized two-photon fluorescence intensity pattern, assuming that plane-polarized beam is reflected from a mirror. Slight aperiodicity of pattern is caused by giant pulse envelope. No single point appears appropriate for a peak-to-background intensity ratio determination. However, peak to background averaged over the round-trip period has the value ≈ 1.6 , indicating a lack of correlation between spectral components. Structure of pattern reflects the detailed pulse structure and is not based on the assumption of subcavities.

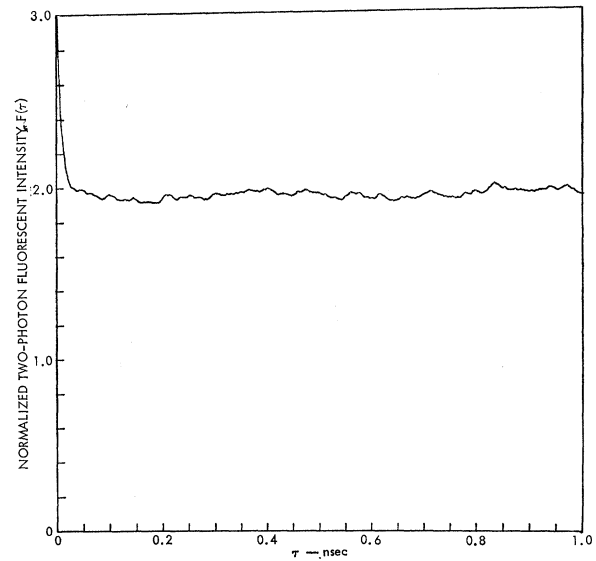


FIG. 10. Normalized two-photon fluorescence intensity pattern for spontaneous emission noise, calculated numerically using the second right-hand term of Eq. (5.2) in Eqs. (7.1) with $T_2=20$ psec, $\Delta t=0.2T_2$, and a time $T=10\,000$ sampling intervals. The background intensity fluctuates about a mean value of 1.95, but the background mean itself will fluctuate from record to record about the value 2.0. This is due to fluctuations in the normalization constant,

$$\int_0^x I^2(t) dt$$

brought about by the finite record length.

where T is the duration of the emission and

$$G(\tau) = \int_0^T I(t+\tau)I(t) dt / \int_0^T I^2(t) dt. \quad (7.1b)$$

Equations (7.1) apply to an experiment in which linearly polarized light is reflected back on itself, and τ measures the delay experienced by light in traveling from some point in the fluorescing fluid to the mirror and back again. A plot of $f(\tau)$ for Fig. 8 is displayed in Fig. 9. The background, it will be noted, contains a well-defined structure. For comparison, the reader's attention is directed to Fig. 10 in which the fluorescence pattern for pure spontaneous emission noise is displayed. Structure has also been observed experimentally in the fluorescence patterns for actively switched lasers.^{9,10} This structure may be attributable to sub-cavities in the laser systems observed, although this explanation seems unlikely in view of the fact that in Ref. 10 different structure is reported for different firings of the same laser, pointing to the possibility that the observed patterns simply reflect the variable pulse structure present in laser emission itself. The background in Fig. 9 appears to fluctuate about a mean value of 1.9. Thus the ratio of the peak-to-background averaged over most of the round trip period is ≈ 1.6 . If the laser field could be represented as a Fourier series of randomly phased normal-mode oscillations, the peak-to-background ratio would have the value 1.5, at least if averaged over an ensemble of measurements. It is difficult to attach any significance to the small difference between the peak-to-background ratios for Fig. 9 and that for the case of randomly phased modes. First of all, the mean background is likely to fluctuate from record to record due to fluctuations in the denominator of Eq. (7.1b) (see Fig. 10). Secondly, a periodic representation does not apply strictly to the nonstationary emission history of a Q -switched laser. If the field were, in fact, periodic, $f(\tau)$ would be periodic with a period equal to the round-trip period, but in Fig. 9 the height of the maximum for τ equal to the round-trip time is slightly less than the 3.0 value at $\tau=0$. This represents the effect of the giant pulse envelope. Measurements for a Q -switched Nd:YAG laser (YAG=yttrium

aluminum garnet) give a peak-to-background ratio of 1.4 ± 0.1 , where the background measurement is taken at a point between the maximum at the mirror and the first subsidiary maximum.⁶¹ In Ref. 54, measurements for a free-running laser showed a Gaussian-shaped fluorescent yield for two overlapping, oncoming beams with a peak value of 2.8 ± 0.2 and a value of 2.0 ± 0.2 far out in the wings. If one picks the first minimum in Fig. 9, the peak-to-background ratio is 1.7, which lies slightly out of the range of the above measurements. However, it is also evident from Fig. 9 that no single point can be selected *a priori* as most suitable for a determination of the peak-to-background ratio. In view of the peak-to-average-background ratio of 1.6, it is to be concluded that the spectral components in Figs. 7 and 8 if not representative of stationary Gaussian noise are at least highly uncorrelated.⁶² This result might be expected in view of the minimal role which pumping plays in the operation of a Q -switched solid-state laser, since it is pumping which brings about the stabilizing characteristics of a self-sustained oscillator in a laser.⁶³

VIII. CONCLUSION

In the past, laser-fluctuation phenomena have been treated theoretically in terms of the statistical properties of an entire ensemble of systems. In the present work, we have demonstrated a method for generating an individual member of such an ensemble, which is what one normally does in performing an experiment. This method is particularly useful for studying the properties of Q -switched laser radiation for which it is found that the pulse structure at high power depends directly on noise fluctuations at low power.

ACKNOWLEDGMENT

The author is indebted to Alex Cecil for much helpful discussion concerning computer programming problems.

⁶¹ S. K. Kurtz and S. L. Shapiro, Phys. Letters **28A**, 17 (1968).

⁶² The possible resemblance of a multimode laser to a Gaussian random source has been noted by L. Mandel and E. Wolf, Rev. Mod. Phys. **37**, 231 (1965).

⁶³ In some ways the role of the rapidly decaying upper level in the saturable absorber is analogous to that of a rapidly acting pump.